Colloidal magnetic gels for the decontamination of limited access metallic surfaces

Hippolyte Pochat-Cottilloux, Fabien Frances, Luc Girard, Aditya Rivonkar, Alban Gossard

Environmental Technology & Innovation 35 (2024) 103688

Contents lists available at ScienceDirect

Environmental Technology & Innovation

journal homepage: www.elsevier.com/locate/eti

Colloidal magnetic gels for the decontamination of limited access metallic surfaces

Hippolyte Pochat-Cottilloux [a], Fabien Frances [a], Luc Girard [b], Aditya Rivonkar [c], Alban Gossard [a,*]

[a] CEA, DES, ISEC, DMRC, Univ. Montpellier, Marcoule, Bagnols-sur-Cèze 30207, France
[b] Univ Montpellier, ICSM, CEA, CNRS, ENSCM, Marcoule, Bagnols-sur-Cèze 30207, France
[c] Subatech Laboratory, IMT Atlantique CNRS/IN2P3 Nantes University, Nantes 44300, France

ARTICLE INFO

Keywords:
Decontamination
Gel
Metal
Nuclear
Ferromagnetic particles

ABSTRACT

Handling nuclear metallic waste is a crucial issue for the nuclear industry, notably by using adapted decontamination processes. Colloidal gels can be applied by spraying for nuclear decontamination of large and plane metallic surfaces, such as walls or floors. However, this implementation mode limits their use for the decontamination of inaccessible or complex geometries surfaces. For that purpose, decontamination magnetic gels have been formulated by incorporating magnetite particles in a pre-synthesized colloidal gel able to decontaminate stainless steel. Such gels can thus be attracted by a magnet, allowing remote application to surfaces with limited access. The presence of magnetite particles does not influence the inherent decontamination properties of the gel, but plays a significant role on the spreading properties by increasing the gel viscosity. Then, a linear relationship between the gel thickness and the decontamination possibilities has been highlighted. Furthermore, as the magnetite particles dissolve in the gel with time, spreading properties, and consequently the decontamination properties, are modified. Finally, a formulation compromise has to be found for a long-term storage of the gels, while maintaining their efficiency.

1. Introduction

The decontamination of solid surfaces is an important issue in the nuclear industry. Particularly, decontamination is required to reduce the activity of certain forms of waste and avoid the generation of large volumes of contaminated final waste. The diversity of the materials involved makes these operations laborious and specific. Among them, metallic wastes, and particularly stainless steel (SS) materials, are critical to decontaminate (Hahm et al., 2023). They are widely produced from the contamination of the primary circuit components within power stations (Rivonkar et al., 2022), processing vessels at reprocessing plants (Barton et al., 2023) or from hot cell walls and floors for example. Thus, different surface geometries have to be considered such as large and plane walls but also small items having complex geometries such as pipes, valves or pumps. On SS, radioactive isotopes can be physically adsorbed onto the surfaces, but also incorporated in an oxide layer due to their contact with strongly corrosive solutions at high temperatures and pressures (Barton et al., 2023; Kerry et al., 2018; Zhong et al., 2021). Consequently, decontamination operations aim to eliminate micron-thick layers to release the contamination. Different technologies have thus been developed over the years for that purpose

* Corresponding author.
E-mail address: alban.gossard@cea.fr (A. Gossard).

https://doi.org/10.1016/j.eti.2024.103688
Received 30 January 2024; Received in revised form 2 May 2024; Accepted 21 May 2024
Available online 22 May 2024

(Zhong et al., 2021; Liu et al., 2022), consisting in physical (high pressure water, ultrasonic techniques…) or chemical (use of liquid reagents, gels/foams, electrochemical techniques…) decontamination processes (Wang et al., 2023; Katona et al., 2022; Rivonkar et al., 2022; Lv et al., 2023; Yoon et al., 2021, 2013; Grebennikova et al., 2021; Kameo et al., 2003).

One technique facilitating the decontamination of SS and producing only a small amount of secondary solid waste is the "vacuumable" gel technology (Gossard et al., 2022). Vacuumable gels are suspension of mineral particles (typically silica or alumina) in a decontamination solution. Due to their viscoelastic properties, such gels form millimeter layers adhered onto surfaces, which induce a prolonged contact with the decontamination solution. This solution is specifically chosen to dissolve the contaminated surface down to few tens of microns to release and absorb the incrusted contamination. Then, the gel dries by evaporation of the solution and fractures into millimetric solid residues, also called flakes, trapping the contamination. These residues are finally easily removable by brushing or vacuuming before being conditioned in adapted immobilization matrixes. This process only produces inorganic solid waste at the end of the operation, meaning that there is no secondary liquid effluent that has to be treated. Vacuumable gels are widely used for the nuclear decontamination of metallic surfaces (Gossard et al., 2022; Jung et al., 2016), but their formulation can also be modulated for multiple applications (Gossard et al., 2021; Gossard and Lepeytre, 2017; Lemesre et al., 2019; Lepeytre et al., 2021; Castellani et al., 2014a, 2014b). Spraying is the most popular application mode for these gels, to treat large and flat surfaces such as the walls or floors. However, this implementation process is not adapted for the decontamination of small objects with complex geometries such as pipes, valves or pumps, or for inaccessible surfaces.

This article describes a new process adapted for the decontamination of limited access surfaces inspired from the formulation of ferrofluids, and particularly ferrogels. Ferrofluids consist in the dispersion of ferromagnetic particles in a liquid solution, forming stable colloidal suspensions sensitive to magnetic fields and useful for medical or heat transfer applications (Rinaldi et al., 2005; Campelj, 2023; Hong et al., 2007). In the presence of a cross-linked polymer, such as poly(vinyl alcohol), in the liquid phase, these fluids are named ferrogels (Zrinyi et al., 1997; Zélis et al., 2013). The polymeric network in the liquid phase provides specific rheological properties to the ferrogels, making them easily shape-controllable and remotely controlled under a magnetic stimulation, extending their implementation possibilities (López-López et al., 2006; Ganguly and Margel, 2020; Lawrence and Rao, 2023). Thus, the addition of ferromagnetic particles in a vacuumable gel leads to a stable dispersion sensitive to magnetic fields and having the specific rheological properties of the vacuumable gels (Gossard et al., 2022). These properties make the gels easily shape-controllable and remotely controlled under a magnetic stimulation, extending their implementation possibilities. Particularly, the addition of Fe_3O_4 magnetite particles in a pre-synthesized vacuumable gel, specifically designed for the decontamination of SS surfaces, was investigated. Then, such gels can be spread by attraction with a magnet, allowing their remote application on limited access surfaces. After decontamination and drying, the produced secondary solid waste containing the ferromagnetic particles can also be recovered with a magnet. The specific objectives of this work are: (i) to introduce a new decontamination process based on a colloidal magnetic gel for the nuclear decontamination of limited access metallic surfaces, (ii) to evaluate the effect of the ferromagnetic particles concentration on both the physicochemical and spreading properties of the magnetic gels and (iii) to highlight the relationship between the gels properties, the deposited thickness and the SS corrosion efficiency of the process.

2. Material and methods

2.1. Materials

A commercial decontamination gel, named ASPIGEL 100E from the FEVDI Company (France), was used in this study. Particles of magnetite (Fe_3O_4, Iron (II, III) oxide powder, Sigma-Aldrich) were added in this gel as ferromagnetic particles. The different operations of gel spreading were performed with a commercial magnet (N829 from Eclipse Magnetics, UK) on 2 millimeter thick 316 L stainless steel (SS) coupons.

2.2. Formulation of the magnetic gels

The magnetic gels were obtained by gently mixing an adapted content of Fe_3O_4 particles with the ASPIGEL 100E. For that, the gel was manually mixed using a plastic spatula until obtaining a creamy like texture. The Fe_3O_4 particles were then added and the gel was

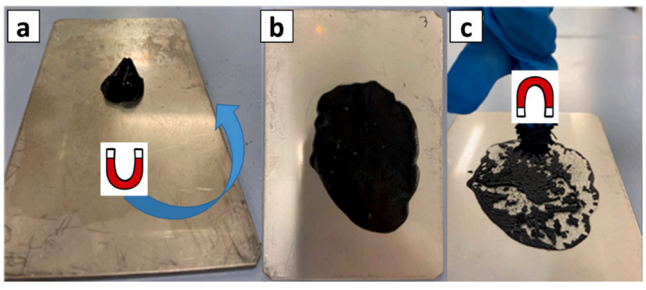

Fig. 1. Different steps of a SS sample simulated decontamination operation using a magnetic gel: (a-b) Manual deposition of a gel drop and spreading of the gel using a magnet, (c) Recovering of the solid flakes obtained after drying using a magnet.

homogenized to well disperse the particles. Finally, the gel was let to rest for 1 day before being used. The different gels are referred to as Gel_x with x being the weight percentage in Fe_3O_4.

2.3. Deposition of the magnetic gels on SS surfaces, drying, solid waste recovery and evaluation of the SS corroded depth

The application protocol of the gel is illustrated Fig. 1. Before all, the SS coupon was washed with water and ethanol, let to dry and weighted using a Secura® 324 Sartorius (Germany) scale having a 10^{-4} g precision. After a slight manual stirring using a spatula, a drop of gel (with a known mass) was deposited on a SS coupon. Then, the commercial magnet was placed on the opposite face of the SS coupon and slowly moved in a circular motion. Due to the presence of the magnetite particles, the gel was spread on the coupon by being attracted by the magnet and adhering to the SS substrate. This operation was performed until the gel was completely spread and no longer moved at the passing of the magnet. To evaluate the gel spreading properties (in $cm^2.g^{-1}$), a picture of the gel layer was taken and its area was determined using ImageJ software (Schneider et al., 2012) and normalized by the mass of gel initially deposited on the surface. With the calculation of the gel density (obtained directly from the densities of the ASPIGEL100E and the magnetite particles, see Supplementary Material), an average gel thickness can be calculated using Eq. (1).

$$th = \frac{m}{S \times d} \tag{1}$$

With th being the average gel thickness, m the deposited mass of gel, S the gel surface after spreading, and d the gel density (depending on the content of magnetite particles).

Then, the gel is left to dry overnight to form millimeter-scale flakes as secondary solid waste. Due to the presence of the magnetite particles, these solid flakes were recovered by attraction with the same commercial magnet. After that, a picture was taken and the percentage of solid recovered by the magnet was determined using ImageJ software. Finally, any residues were removed using a wet wipe.

After washing the coupons using water and ethanol, they were let to dry and weighted again. Noteworthy it was ensured that the wet wipe has no impact on the mass loss by comparing the mass of a coupon before and after using the wet wipe, without previous application of gel. The mass loss was calculated and the corroded SS depth was evaluated (and considered as related to the decontamination efficiency), using the following equation:

$$Corroded\ depth = \frac{\Delta m}{S \times d} \tag{2}$$

With Δm being the mass loss, S the surface covered by the gel and d the SS density (fixed at 8 $g.cm^{-3}$).

For each gel, five trials were performed for the sake of reproducibility and the different results are given as averages. Moreover, an experiment was also performed with the ASPIGEL 100E without magnetite particles to compare its efficiency with the magnetic gels of this study. For that, the ASPIGEL 100E was laid on the SS substrate with a controlled area and a millimeter thickness (see Supplementary Material).

2.4. Characterizations

The magnetite particles were characterized by different techniques. Transmission electron images were taken using a Hitachi (Japan) HT7800 microscope. Infrared (IR) spectra was obtained on a Shimadzu (Japan) IRS Spirit device. Zeta-potentials were measured by using a Malvern (UK) Zetasizer Ultra Red. The particles elementary composition was determined by X-ray Fluorescence performed with a Bruker (USA) S8 Tiger device. The rheological properties of the gels were characterized by using a TA instruments (USA) Discovery Hybrid Rheometer (DHR 1) with a vane geometry. First, a shearing at 1 s^{-1} was applied for 1 minute. After that, this shearing was immediately decreased to a very low value (0.015 s^{-1}) and the viscosity was followed with time for 45 minutes. The spreading of the gel as well as the percentage of recovered solid flakes using a magnet was evaluated by image treatment. Pictures were taken after the gel spreading and after the solid recovering and analysed using Image J software to calculate the area of the gel layer and the percentage of recovered flakes. X-ray diffraction (XRD) analysis was carried out using a D8 Advance, Bruker (USA) XRD device with a Cu Kα-1 radiation source (λ = 1.5406 Å). XRD measurements were recorded under the following conditions: 10° - 100° 2theta, a step size of 0.01°, and a scan speed of 4.5 sec/step. The XRD patterns were analyzed using Bruker Diffrac Eva software (Version 4.3.1.2) and the different phases were identified using the Crystallographic Information Files (CIF) of the Crystallography Open Database (COD, Rev 173445) (Grazulis et al., 2012). A beam knife was used to reduce the background scattering at low angles. Portable X-ray Fluorescence (pXRF) spectra were collected on SS samples with a Bruker (USA) TRACR 5i handheld unit. The TRACER 5i unit was operated while facing up with the metallic sample in contact with the nose of the unit. Data collection was controlled through Bruker *Artax* software. The pXRF operating conditions were 40 kV, 5.1 μA for 10 s with a Rh anode. The beam was collimated down to 8 mm. A Ti 25 μm Al 200 μm filter was used to reduce the background. The evolution of the iron concentration in a liquid decontamination solution due to the dissolution of the magnetite particles was determined using an inductively coupled plasma - optical emission spectrometry (ICP-OES, ThermoFisher (USA) Scientific iCAP 6000 Series).

3. Results and discussion

3.1. Addition of ferromagnetic particles to displace the gel using a magnet

3.1.1. Characterization of the magnetite particles

The magnetite particles were finely characterized using different techniques (see Supplementary Material). The size of the particles determined on TEM images shows a large distribution in diameter and an average size of 178 ± 71 nm. As ferrofluids refer to fluids containing nanoscale (5–15 nm) ferromagnetic particles, gels containing these particles will not be theoretically considered as ferrofluids (Rinaldi et al., 2005; Campelj, 2023). Thus, and despite they behave as ferrofluids, the gels formulated in this work are named "magnetic gels". The X-ray diffractogram of the powder presents a well crystallized magnetite phase with a crystallite size of 143 nm. These magnetite particles are composed of 70.2 wt% of Fe with some Mn and Si impurities (0.3 and 0.1 wt% respectively), and the IR spectra presents the characteristic band of magnetite (Fe_3O_4) at 590 cm^{-1} (Ivashchenko et al., 2016). The particles are positively charged in acidic media and negatively in alkaline media, and their isoelectric point was determined at pH = 7.25.

3.1.2. Rheological behavior

Different weight percentages of magnetite particles were added to the gel (5, 8.5 and 13 wt%). To better understand the gels behavior and anticipate their spreading properties with a magnet, the rheological properties of the gels were analysed and compared with the behavior of the gel without particles (Gel_0). First, a shear rate of 1 s^{-1} was applied as a stimulation of the gel equivalent to a manual shearing and its deposition from its container on a surface. During this shearing phase, the gel viscosity decreases, notably because the silica particles network (allowing the "gel-state") is broken and the silica particles self-organize in the direction of the shearing flow (Gossard et al., 2017). This shear-thinning feature is typical of mineral gels (Gossard et al., 2017, 2021, 2022; Lepeytre et al., 2021) and is not affected by the presence of the magnetite particles. Then, this shearing was suddenly decreased to a very low value (0.015 s^{-1}) to simulate the gel at rest directly after the manual deposition. The viscosity was followed with time during this second step and its evolution is shown in Fig. 2.

For the four gels, a strong increase of the viscosity is immediately observed during the first minutes, before a viscosity plateau is reached. Indeed, silica-based colloidal gels are thixotropic fluids and, during the period following the shearing, the silica particles reorganize themselves to recreate a viscous network and strengthen the suspension into a gel again. At equilibrium, a few amount of particles (5 wt%) does not significantly impact the gel viscosity. Then, the higher the magnetite particles' concentration in the gel formulation, the higher the viscosity at the plateau, and consequently the overall viscosity of the gel. Indeed, adding magnetite particles leads to a larger amount of solid volume in the gel formulation and consequently to a more compact gel-state (Zhou et al., 2001; Hong et al., 2007; Giwa et al., 2021).

3.1.3. Spreading tests on a stainless steel substrate using a magnet

Spreading tests were performed using a magnet with a common and reproducible protocol (Fig. 1). From these experiments, the gel spreading, the gel deposited thickness, the corroded metal depth and the percentage of recovered flakes using the magnet were determined and are reported in Table 1.

Fig. 3 highlights the influence of the magnetite particles content in the gels on their spread thickness as well as their SS corrosion efficiencies.

Higher contents of ferromagnetic particles induce lower spreading properties. Particularly, at a given mass of deposited gel, the

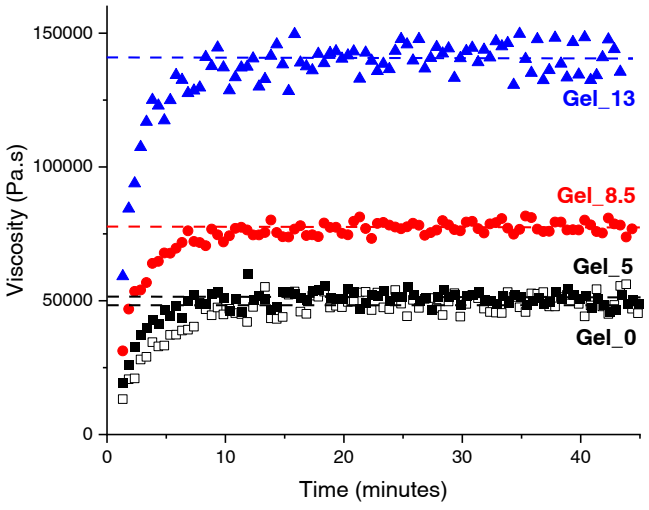

Fig. 2. Viscosity recovery with time at a shear rate of 0.015 s^{-1} after a 1 minute shearing step at 1 s^{-1} for the gel with no particles (Gel_0, empty black squares), Gel_5 (filled black squares), Gel_8.5 (red circles) and Gel_13 (blue triangles).

Table 1
Summary of the data determined from the different experiments using the Gel_x.

Gel	Calculated density	Aging	Gel spreading ($cm^2.g^{-1}$)	Gel deposited thickness (mm)	Corroded metal depth (µm)	Percentage of recovered flakes (%)
Gel_5	1.35	/	5.90 +/- 0.39	1,28 +/- 0.08	0.69 +/- 0.08	91.7 +/- 0.8
		1 week	8.51 +/- 0.39	0.88 +/- 0.04	0.35 +/- 0.02	95.5 +/- 0.4
		2 weeks	8.80 +/- 0.42	0.85 +/- 0.04	0.28 +/- 0.02	91.6 +/- 0.7
		3 weeks	9.36 +/- 0.40	0.80 +/- 0.03	0.21 +/- 0.02	90.0 +/- 0.9
Gel_8.5	1.39	/	5.38 +/- 0.37	1,37 +/- 0.08	0.59 +/- 0.04	92.6 +/- 0.4
		1 week	6.16 +/- 0.22	1.18 +/- 0.04	0.36 +/- 0.02	91.8 +/- 0.8
		2 weeks	6.51 +/- 0.21	1.11 +/- 0.04	0.27 +/- 0.02	96.8 +/- 0.5
		3 weeks	7.06 +/- 0.27	1.03 +/6 0.04	0.20 +/- 0.01	95.6 +/- 0.3
Gel_13	1.44	/	5.00 +/- 0.16	1,39 +/- 0.04	0.58 +/- 0.02	91.5 +/- 0.8

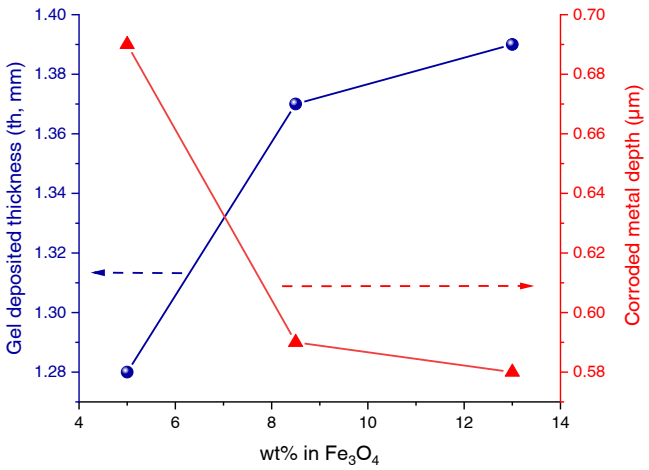

Fig. 3. Influence of the content of ferromagnetic particles added in the gels on their spreading properties and corrosion efficiencies.

area of the gel layer spread using the magnet decreases with the increase of the magnetite particle concentration and, as a result, the gel deposited thickness is higher. Indeed, although the magnetic response of the gel should be higher due to the presence of more ferromagnetic particles (López-López et al., 2006; Minuti et al., 2022; Küster et al., 2023), the viscosity of the gel increases, as shown in Fig. 2, which has a strong impact on the gel displacement possibility. There is consequently a direct relationship between the gel magnetic sensibility, their rheological properties and the gel deposited thickness. Considering these results, a small amount of magnetite particles is enough to spread the gel to a satisfying millimeter thickness and thus a large area.

3.1.4. Secondary solid waste recovery and evaluation of the corrosion efficiency

After gel drying, millimeter sized solid residues were obtained (Fig. 1). Such flakes are formed by the evaporation of the liquid phase of the gel, inducing the aggregation of the solid particles and then cracks in the structure due to capillary forces (Gossard et al., 2022; Sobac et al., 2019; Lilin and Bischofberger, 2022). The final residues are mainly composed of the silica and magnetite particles, but also of the different elements composing the metallic layer, which has been dissolved and absorbed in the gel. Note that no specific influence of the gel formulation was observed on the size and shape of the flakes. The drying step and the formation of the solid residues are thus controlled by the silica particles initially present in the gel rather than by the added magnetite particles. Moreover, the differences in the spread gel thicknesses are not significant enough to observe any variation in the solid size as it could be expected (Gossard and Lepeytre, 2017). Capillary forces also trigger a delamination phenomenon on the edges of the flakes, leading to their detachment from the substrate (Gossard et al., 2022; Sarkar and Tirumkudulu, 2011). Then, thanks to the presence of the magnetite particles, they can be easily attracted by a magnet, as shown on Fig. 1c. In this way, the vast majority of the flakes (more than 90% for each formulation, see Table 1) can be recovered with the magnet used in this study. The remaining residues mainly come from thinner gel thicknesses on the edges of the gel layer, leading to smaller flakes adhered more strongly to the surface (Gossard and Lepeytre, 2017). They can be finally eliminated using a wet wipe or by a slight washing with water and ethanol, before the SS substrate was weighed to determine the mass lost and consequently the SS corrosion depth using Eq. (2). The evolution of the corroded SS depth as a function of the content of magnetic particles is shown Fig. 3. First, note that the corrosion efficiency of few tens of microns is of the same order of magnitude for the magnetic gels than for the pristine ASPIGEL 100E, and is in agreement with the specification of the gel

supplier (see Supplementary Material). Then, there is a significant influence of the concentration of magnetite particles on the overall efficiency of the process. Indeed, while increasing the content of magnetite particles in the gel leads to larger layer thicknesses, the corrosion efficiency of the stainless steel surface after gel drying decreases. However, a thicker gel layer enables a larger decontamination solution volume at the surface of the SS and consequently should lead to a longer chemical reaction and a deeper corrosion, but the opposite is observed. In this way, the presence of too many magnetite particles in the gel formulation has negative effects on both the spreading properties of the gel and also its decontamination efficiency. This latter observation may be explained by a chemical evolution of the decontamination solution, initially designed to dissolve SS surfaces, in the presence of the magnetite particles (Banerjee et al., 2023; Rivonkar et al., 2022). To validate this hypothesis, a few grams of magnetite particles were dispersed in different batches of a FEVDIRAD liquid solution (detailed protocol presented in Supplementary Material). According to the safety data sheet, this solution, commercialized by the FEVDI Company, has a chemical composition close to the decontamination solution of the ASPIGEL 100E, i.e. HNO_3 and Ce(IV). Then, the ionic iron concentration in solution increases with the contact time between the particles and the solution (see in Supplementary Material), confirming that there is a chemical reaction leading to the consumption of the decontamination solution and the dissolution of the magnetite particles.

After drying and elimination of the solid residues, the SS substrates were washed with water and ethanol. A dark coloration of the SS appeared at the end of the process. pXRF and XRD analyses were performed on the different samples and the results are given in Fig. 4.

The initial SS substrate is mainly composed of Fe, Ni, Cr and Mo, as illustrated by its pXRF analysis. The difference between the pXRF spectra of the SS substrate before and after the magnetic gel treatment shows a decrease of the amount of Fe, which could be characteristic of the formation of a thin oxide layer and consistent with the visual color variation.

The X-ray diffractograms show the presence of the fcc structure of Fe, or Austenite (CIF: 9015071), as the main crystalline phase

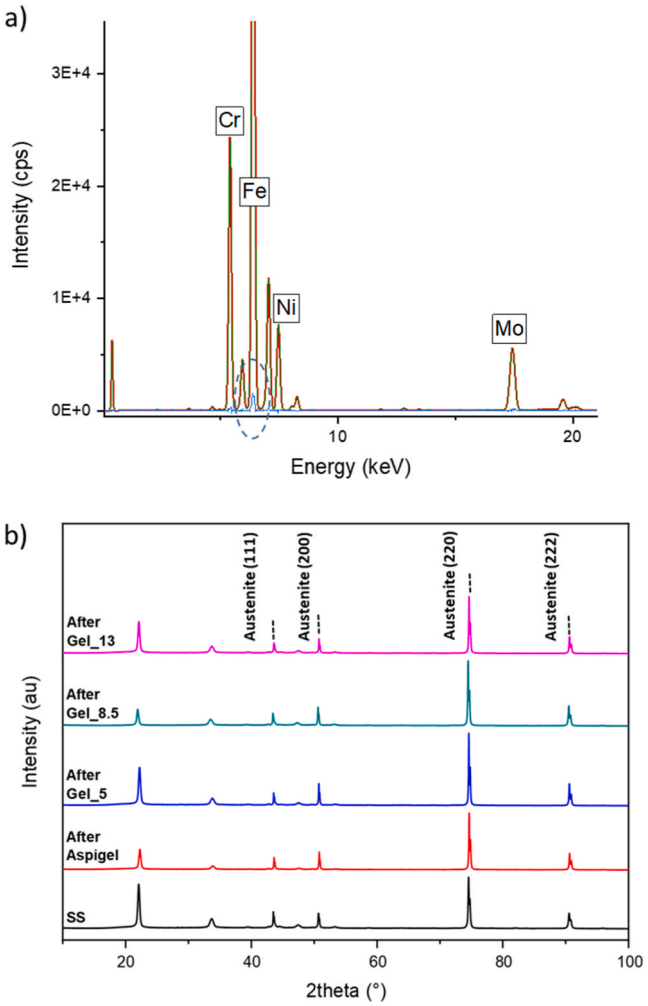

Fig. 4. (a) X-ray fluorescence and (b) X-ray diffraction analyses of the SS coupons treated using magnetic gels. For X-ray fluorescence, the initial sample is plotted in red and the sample treated by Gel_13 is shown in green as an illustrating example. As data almost superimposed, the pink plot corresponds to the difference between both spectra.

(Dadfar et al., 2007) in all samples before and after the gel treatment. This highlights that the treatment does not significantly alter the bulk of the SS substrate. Some other small peaks are also observed, but their intensity is very slight in comparison to the Austenite base metal and their precise assignment may rise to identification errors under current configuration. These peaks may correspond to different oxide phases, such as Fe_3O_4, Fe_2NiO_4 or Cr_2FeO_4, which are generally expected on such substrates after contact with aqueous corrosive solutions (Rivonkar et al., 2022; Panter et al., 2006). Thus, the modification of the oxide layer is observed by pXRF and not visible by XRD. Indeed, the thin oxide layer is certainly smaller than the penetration depth of the X-Ray beam, which is of the order of magnitude of 1 μm. Finally, there is no difference between the surface treated with the ASPIGEL 100E or with the different magnetic gels, illustrating that the presence of ferromagnetic particles does not impact the mechanism of decontamination.

3.2. Aging of the gel and influence on the decontamination possibilities

As that the magnetite particles react with the ASPIGEL 100E decontamination solution, it is worth investigating the influence of the aging on the rheological, spreading and decontamination properties of the gels. Note that these experiments were performed only on the gels Gel_5 and Gel_8.5. Indeed, Gel_8.5 and Gel_13 present similar performances (Fig. 3), but with the latter producing a larger secondary waste volume due to its higher content in magnetite particles.

3.2.1. Evolution of the rheological properties with time

The rheological analysis protocol previously described was performed on the Gel_5 and Gel_8.5 at different aging times (1, 2 and 3 weeks). After application of a shear rate of 1 s^{-1}, the viscosity was followed over time at a shear rate of 0.015 s^{-1} for 45 minutes until reaching a plateau. Fig. 5 presents the evolution over time of the plateau viscosity values of the considered gels (the complete data of the viscosity recovery are given in Supplementary Material).

The aging of the gels induces a significant drop of their viscosities. Indeed, as shown above, Fe_3O_4 particles react and dissolve with the ASPIGEL 100E decontamination solution. This leads to a diminution of the solid concentration in the gel, which has a strong influence on the gel viscosity (Zhou et al., 2001; Hong et al., 2007; Giwa et al., 2021): the lower the content of particles in the gel, the lower the viscosity of the gel.

3.2.2. Influence of aging on the spreading properties

The spreading efficiencies of the Gel_5 and Gel _8.5 were evaluated at different storage times (Fig. 6).

For the two gels, the gel deposited thickness for a given mass decreases with the storage time, meaning their spreading properties are improved. Moreover, the spreading properties are more significantly affected during the first week of aging. Indeed, as observed in the Supplementary Material, the dissolution rate of the Fe_3O_4 particles is higher during the first days of contact. This decrease of the gel deposited thickness is in accordance with the drop in viscosity. Even if some Fe_3O_4 particles are dissolved, which certainly reduces the magnetic response of the gels, the drop in viscosity has a stronger impact on the gel spreading properties. Consequently, a small concentration of ferromagnetic particles is sufficient for the application of the gel using a magnet.

For the first experiment performed at t = 0, the gel thickness is slightly larger for the Gel_8.5 than for the Gel_5, while this is the opposite for the SS corrosion depth. These differences are quite tenuous but can be explained by the chemical reaction between the Fe_3O_4 particles and the decontamination solution. Indeed, as the gels were evaluated with one day after their formulation, the Gel_8.5 may have consumed more decontamination reagents than the Gel_5. This is confirmed by the evolution over time. The lower gel

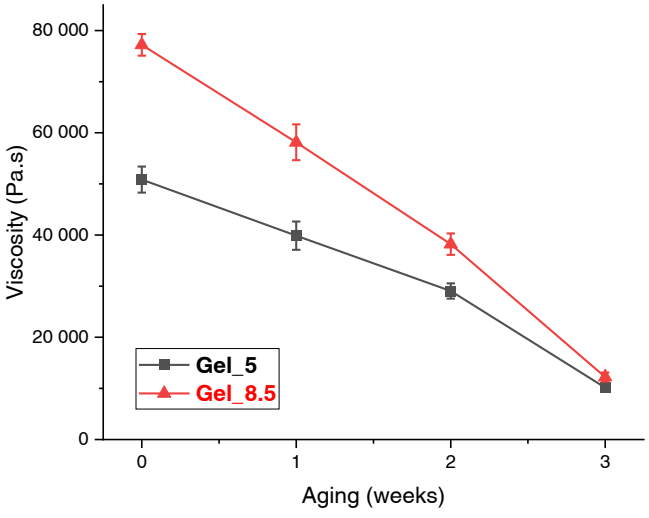

Fig. 5. Evolution over time of the viscosity plateau values obtained at a shear rate of 0.015 s^{-1} for the Gel_5 (black squares) and Gel_8.5 (red triangles).

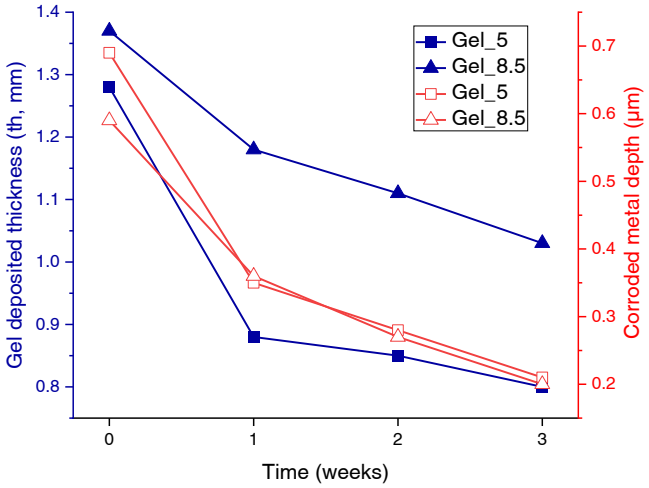

Fig. 6. Influence of the aging of the Gel_5 (square symbols) and the Gel_8.5 (triangle symbols) on their deposited thicknesses (blue full symbols) and their corrosion efficiency (red empty symbols).

thicknesses obtained with aging has a direct influence on the corrosion depth of the SS due to the lower volume of decontamination solution at the contact of the SS surface. Moreover, although the gel deposited layers are thinner for Gel_5, the metal corrosion depth remains within the same order of magnitude for the two gels. The presence of a larger amount of magnetite particles in the Gel_8.5 induces a more significant drop in the gel efficiency due to the consumption of the decontamination solution. Nevertheless, for both gels with storage times longer than 1 week, the dissolved layer of SS is less than 0.3 µm. This could limit the application of such gels, depending on the thickness of the oxidized layer to remove.

3.3. Relationship between the gel deposited thickness and the metal corrosion efficiency

The different data acquired in this study (including the repeatability tests) are given in Fig. 7, which represents the evolution of the metal corrosion efficiency of gel layers as a function of their deposited thickness.

This graph highlights a linear relationship between the gel deposited thickness and the dissolved SS layer depending on the gel formulation and aging. For fresh gels and large gel thicknesses ($>$ 1 mm), the dissolved SS layers are higher than 0.4 µm and the slope is steep. Indeed, for larger gel thicknesses, the volume of decontamination solution is more important locally and the drying time is consequently longer, inducing a continuous supply of chemical reagent at the gel-SS interface and a deeper corrosion of the surface (Gossard and Lepeytre, 2017; Lemesre et al., 2019). The increase of the concentration in magnetite particles in the gel leads to a decrease of the slope of the linear tendency. This could come from the more important consumption of the decontamination solution by reaction with the magnetite. Moreover, at a given mass, the presence of a higher solid content in the gel formulation induces a lower volume of decontamination solid deposited on a given surface area.

As described above, the aging of the Gel_5 and Gel_8.5 leads to a drop in their viscosity and thus better spreading properties, lower gel thicknesses and then thinner dissolved SS layers, which is confirmed in Fig. 7. Moreover, the linear tendency is less steep after one week aging. Indeed, thinner gel thicknesses will induce shorter drying time and the aggregation of the colloidal particles (Gossard and Lepeytre, 2017). This leads to the freezing of the whole system and the limitation of the SS dissolution. Then for aging time higher than one week, the gel thicknesses remain of the same order of magnitude but, at a given thickness, the dissolved SS layer is lower. This is consistent with the consumption of the decontamination solution due to the reaction with the magnetite particles. Finally, comparing the evolution of the Gel_5 and Gel_8.5 with time, Gel_5 spreads better than Gel_8.5, but the linear relationship with the SS dissolution layer is similar. Consequently, for a given area to be decontaminated, Gel_5 appears to be better suited. Indeed, even if a partial dissolution of the magnetite particles occurs, a small amount is enough for the gel to be efficiently spread. Moreover, this leads to a lower volume of secondary waste to be conditioned at the end of the process.

3.4. Practical applications and future research prospects

This new decontamination process has been specifically developed for the nuclear decontamination of limited access metallic surfaces. As the nuclear industry produces large volume of metallic waste, this process can be used to decontaminate small objects with complex geometries, such as the internal surface of pipes, valves or pumps, and thus facilitate the management of such nuclear waste. Moreover, this process may allow the remote application of decontamination gel in hardly accessible zones, for maintenance operation for example.

This study has shown that the efficiency of the “magnetic gel” process is directly related to the spreading properties of the gel. Thus, to better control the gel application, two main perspectives have been identified. First, the physicochemical properties of the

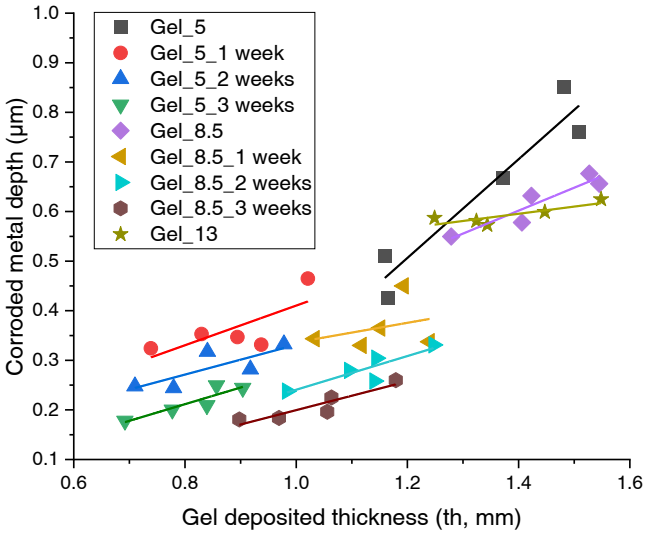

Fig. 7. Evolution of the corroded SS depth after the decontamination operation depending on the thickness of the deposited gel layer. Linear fits are indicated as guidelines for the eyes.

ferromagnetic particles could be studied. Indeed, other natures of particles may present higher magnetic responses, allowing to both better spread the gel and limit the amount of generated secondary waste. Particles having a better chemical resistance in very acidic and oxidizing solutions may also be considered for an optimized preservation of the gel. Moreover, the influence of the type of magnet was not considered in this work. It may reasonably be assumed that the spreading of a gel formulation is also depending on the geometry and the power of the magnet.

4. Conclusions

Colloidal magnetic gels have been developed for the nuclear decontamination of metallic surfaces. Such gels can be moved and spread using a magnet. After drying, the solid residues containing the contamination can also be recovered by the magnet. The decontamination process can thus be remotely implemented to apply the gels on limited access surfaces.

More particles in the formulation increases the gel viscosity, and consequently does not particularly improve its spreading properties. As the decontamination performance depends on the gel spreading, a linear relationship between the gel thickness and the dissolved SS layer has been highlighted.

As magnetite particles dissolve with time in the gel, spreading properties as well as the decontamination efficiency are modified, and a formulation compromise has to be found for a long-term storage of the product. For that purpose, only small amounts of magnetite are enough to spread the gel, without significantly consuming the decontamination solution.

CRediT authorship contribution statement

Luc Girard: Writing – review & editing, Resources, Investigation. **Aditya Rivonkar:** Writing – review & editing, Resources, Investigation. **Alban Gossard:** Writing – original draft, Visualization, Validation, Supervision, Formal analysis, Data curation. **Hippolyte Pochat-Cottilloux:** Methodology, Investigation, Conceptualization. **Fabien Frances:** Investigation, Conceptualization.

Declaration of Competing Interest

The authors declare the following financial interests/personal relationships which may be considered as potential competing interests: Alban Gossard reports financial support was provided by European Union. If there are other authors, they declare that they have no known competing financial interests or personal relationships that could have appeared to influence the work reported in this paper.

Data availability

Data will be made available on request.

Acknowledgments

This project has received funding from the European Union's Horizon 2020 research and innovation programme for Nuclear Fission

and Radiation Protection Research (Call NFRP-2019–2020) under grant agreement No. 945098 (PREDIS). The authors thank Dr. Tomo Suzuki-Muresan for help performing XRD characterizations as well as the SON Company for help characterizing of the magnetite particles.

Appendix A. Supporting information

Supplementary data associated with this article can be found in the online version at doi:10.1016/j.eti.2024.103688.

References

Banerjee, A., Choi, W., Choi, B.S., Park, S., Kim, S.B., 2023. Evaluation of dissolution characteristics of magnetite in an inorganic acidic solution for the PHWR system decontamination. Nucl. Eng. Technol. 55, 1892–1900.
Barton, D.N.T., Grebennikova, T., Denman, A.E., Carey, T., Engelberg, D.L., Sharrad, C.A., 2023. Long-term aqueous contamination of stainless steel in simulant nuclear reprocessing environments. J. Nucl. Mater. 583.
Barton, D.N.T., Johnson, T., Callow, A., Carey, T., Bibby, S.E., Watson, S., Engelberg, D.L., Sharrad, C.A., 2023. A review of contamination of metallic surfaces within aqueous nuclear waste streams. Prog. Nucl. Energy 159.
Campelj, S., 2023. Rheology of aqueous ferrofluids: transition from a gel-like character to a liquid character in high magnetic fields. Chemengineering 7.
Castellani, R., Poulesquen, A., Goettmann, F., Marchal, P., Choplin, L., 2014. A topping gel for the treatment of nuclear contaminated small items. Nucl. Eng. Des. 278, 481–490.
Castellani, R., Poulesquen, A., Goettmann, F., Marchal, P., Choplin, L., 2014. Efficiency enhancement of decontamination gels by a superabsorbent polymer. Colloids Surf. A Physicochem. Eng. Asp. 454, 89–95.
Dadfar, M., Fathi, M.H., Karimzadeh, F., Dadfar, M.R., Saatchi, A., 2007. Effect of TIG welding on corrosion behavior of 316L stainless steel. Mater. Lett. 61, 2343–2346.
Ganguly, S., Margel, S., 2020. Review: remotely controlled magneto-regulation of therapeutics from magnetoelastic gel matrices. Biotechnol. Adv. 44.
Giwa, S.O., Sharifpur, M., Goodarzi, M., Alsulami, H., Meyer, J.P., 2021. Influence of base fluid, temperature, and concentration on the thermophysical properties of hybrid nanofluids of alumina-ferrofluid: experimental data, modeling through enhanced ANN, ANFIS, and curve fitting. J. Therm. Anal. Calorim. 143, 4149–4167.
Gossard, A., Frances, F., Aloin, C., 2017. Rheological properties of TiO2 suspensions varied by shifting the electrostatic inter-particle interactions with an organic co-solvent. Colloids Surf. A Physicochem. Eng. Asp. 522, 425–432.
Gossard, A., Frances, F., Turc, H.A., 2022. Method for Treating Surfaces or Gaseous Media Using a Ferromagnetic Gel. Patent, WO2022/184996.
Gossard, A., Frances, F., Aloin, C., Penavayre, C., Fabregue, N., Lepeytre, C., 2021. Effect of surfactant concentration on the long-term properties of a colloidal Chemical, Biological and Radiological (CBR) decontamination gel. Fluids 6.
Gossard, A., Lepeytre, C., 2017. An innovative green process for the depollution of Cr(VI)-contaminated surfaces using TiO2-based photocatalytic gels. J. Environ. Chem. Eng. 5, 5573–5580.
Gossard, A., Lilin, A., Faure, S., 2022. Gels, coatings and foams for radioactive surface decontamination: state of the art and challenges for the nuclear industry. Prog. Nucl. Energy 149.
Grazulis, S., Daskevic, A., Merkys, A., Chateigner, D., Lutterotti, L., Quiros, M., Serebryanaya, N.R., Moeck, P., Downs, R.T., Le Bail, A., 2012. Crystallography Open Database (COD): an open-access collection of crystal structures and platform for world-wide collaboration. Nucleic Acids Res. 40, D420–D427.
Grebennikova, T., Jones, A.N., Sharrad, C.A., 2021. Electrochemical decontamination of irradiated nuclear graphite from corrosion and fission products using molten salt. Energy Environ. Sci. 14, 5501–5512.
Hahm, I., Kim, D., Ryu, H.J., Choi, S., 2023. A multi-criteria decision-making process for selecting decontamination methods for radioactively contaminated metal components. Nucl. Eng. Technol. 55, 52–62.
Hong, R.Y., Pan, T.T., Han, Y.P., Li, H.Z., Ding, J., Han, S.J., 2007. Magnetic field synthesis of Fe_3O_4 nanoparticles used as a precursor of ferrofluids. J. Magn. Magn. Mater. 310, 37–47.
Hong, R.Y., Ren, Z.Q., Han, Y.P., Li, H.Z., Zheng, Y., Ding, J., 2007. Rheological properties of water-based Fe_3O_4 ferrofluids. Chem. Eng. Sci. 62, 5912–5924.
Ivashchenko, O., Jurga-Stopa, J., Coy, E., Peplinska, B., Pietralik, Z., Jurga, S., 2016. Fourier transform infrared and Raman spectroscopy studies on magnetite/Ag/antibiotic nanocomposites. Appl. Surf. Sci. 364, 400–409.
Jung, C.H., Choi, W.K., Moon, J.K., 2016. Effect of chemical formulations for uranium decontamination by chemical gels. Asian J. Chem. 28, 1285–1287.
Kameo, Y., Nakashima, M., Hirabayashi, T., 2003. Dry flowing abrasive decontamination technique for-pipe systems with swirling air flow. Nucl. Technol. 144, 76–82.
Katona, R., Rivonkar, A., Locskai, R., Bator, G., Abdelouas, A., Somlai, J., Kovacs, T., 2022. Tafel-analysis of the AP-CITROX decontamination technology of Inconel alloy 690. Appl. Radiat. Isot. 181.
Kerry, T., Banford, A.W., Bower, W., Thompson, O.R., Carey, T., Mosselmans, J.F.W., Ignatyev, K., Sharrad, C.A., 2018. Uranium contamination of stainless steel in nuclear processing plants. Ind. Eng. Chem. Res. 57, 3957–3962.
Küster, M., Nadasi, H., Eremin, A., Bostjancic, P.H., Ludwig, F., 2023. Magnetic-field dependence of the magnetic dynamics of barium hexaferrite nanoplatelet suspensions. J. Magn. Magn. Mater. 588.
Lawrence, M.B., Rao, R.K., 2023. Structure of water in poly(vinyl alcohol)-based ferrogels: effect of carbonyl iron concentration. J. Polym. Res. 30.
Lemesre, L., Frances, F., Grandjean, A., Gossard, A., 2019. Hybrid colloidal suspensions tailored as gels to remove radioactive bitumen stains. J. Environ. Manag. 232, 660–665.
Lepeytre, C., Frances, F., Charvolin, M.S., Ludwig, A., Le Toquin, E., Comoy, E., Grandjean, A., Gossard, A., 2021. Colloidal gel as an efficient process to treat Chemical, Biological, Radiological (CBR) and prion contaminated solid surfaces. Chem. Eng. Sci. 246.
Lilin, P., Bischofberger, I., 2022. Criteria for crack formation and air invasion in drying colloidal suspensions. Langmuir 38, 7442–7447.
Liu, S.Y., He, Y.Y., Xie, H.H., Ge, Y.J., Lin, Y.S., Yao, Z.T., Jin, M.Q., Liu, J., Chen, X.Y., Sun, Y.H., Wang, B.H., 2022. A state-of-the-art review of radioactive decontamination technologies: facing the upcoming wave of decommissioning and dismantling of nuclear facilities. Sustainability 14.
López-López, M.T., Kuzhir, P., Lacis, S., Bossis, G., González-Caballero, F., Durán, J.D.G., 2006. Magnetorheology for suspensions of solid particles dispersed in ferrofluids. J. Phys. Condens. Matter 18, S2803–S2813.
Lv, H.T., Gao, J.Z., Chen, J.Q., Li, T.Y., Liang, Y., Hu, B., Ma, F.Q., Xue, Y., Yan, Y.D., 2023. Molten salts for efficient removal of radioactive contaminants from stainless steel surface: mechanisms and applications. Environ. Res. 239.
Minuti, A.E., Stoian, G., Herea, D.D., Radu, E., Lupu, N., Chiriac, H., 2022. Fe-Cr-Nb-B ferrofluid for biomedical applications. Nanomaterials 12.
Panter, J., Viguier, B., Cloué, J.M., Foucault, M., Combrade, P., Andrieu, E., 2006. Influence of oxide films on primary water stress corrosion cracking initiation of alloy 600. J. Nucl. Mater. 348, 213–221.
Rinaldi, C., Chaves, A., Elborai, S., He, X.W., Zahn, M., 2005. Magnetic fluid rheology and flows. Curr. Opin. Colloid Interface Sci. 10, 141–157.

Rivonkar, Aditya, Katona, Richárd, Robin, Mathurin, Suzuki-Muresan, Tomo, Abdelouas, Abdessalam, Mokili, Marcel, Bátor, Gergő., Kovács, Tibor, 2022. Optimisation of the chemical oxidation reduction process (CORD) on surrogate stainless steel in regards to its efficiency and secondary wastes. Front. Nucl. Eng. 1.
Sarkar, A., Tirumkudulu, M.S., 2011. Delamination of drying nanoparticle suspensions. Soft Matter 7, 8816–8822.
Schneider, C.A., Rasband, W.S., Eliceiri, K.W., 2012. NIH Image to ImageJ: 25 years of image analysis. Nat. Methods 9, 671–675.
Sobac, B., Colinet, P., Pauchard, L., 2019. Influence of Benard-Marangoni instability on the morphology of drying colloidal films. Soft Matter 15, 2381–2390.
Wang, Q., Wang, F.S., Cai, C., Chen, H., Ji, F., Yong, C., Liao, D.S., 2023. Laser decontamination for radioactive contaminated metal surface: a review. Nucl. Eng. Technol. 55, 12–24.
Yoon, S.B., Kim, C.K., Jung, C.H., Choi, B.S., Choi, W.K., Lee, K.W., Moon, J.K., 2013. Effect of alkyl alcohol on viscosity of silica-based chemical gels for decontamination of radioactive contaminations. Asian J. Chem. 25, 7023–7027.
Yoon, I.H., Yoon, S.B., Sihn, Y., Choi, M.S., Jung, C.H., Choi, W.K., 2021. Stabilizing decontamination foam using surface-modified silica nanoparticles containing chemical reagent: foam stability, structures, and dispersion properties. RSC Adv. 11, 1841–1849.
Zélis, P.M., Muraca, D., Gonzalez, J.S., Pasquevich, G.A., Alvarez, V.A., Pirota, K.R., Sánchez, F.H., 2013. Magnetic properties study of iron-oxide nanoparticles/PVA ferrogels with potential biomedical applications. J. Nanopart. Res. 15.
Zhong, L., Lei, J.H., Deng, J., Lei, Z.Y., Lei, L., Xu, X.S., 2021. Existing and potential decontamination methods for radioactively contaminated metals-a review. Prog. Nucl. Energy 139.
Zhou, Z.W., Scales, P.J., Boger, D.V., 2001. Chemical and physical control of the theology of concentrated metal oxide suspensions. Chem. Eng. Sci. 56, 2901–2920.
Zrinyi, M., Barsi, L., Buki, A., 1997. Ferrogel: a new magneto-controlled elastic medium. Polym. Gels Netw. 5, 415–427.